Eur. Phys. J. B **23**, 29–36 (2001)

THE EUROPEAN PHYSICAL JOURNAL B

EDP Sciences

Magnetic structure and anisotropy of YFe_6Ga_6 and $HoFe_6Ga_6$

O. Moze[1,a], J.M. Cadogan[2], Y. Janssen[3], F.R. de Boer[3], K.H.J. Buschow[3], and S.J. Kennedy[4]

[1] INFM, Dipartimento di Fisica, Università di Modena e Reggio Emilia, Via G. Campi 213/a, Modena, 41100, Italy
[2] School of Physics, University of NSW, Sydney, 2052, Australia
[3] Van der Waals-Zeeman Institut, Universteit van Amsterdam, Valckenierstraat 65, 1018 XE, Amsterdam, The Netherlands
[4] Neutron Scattering Group, Australian Institute of Nuclear Science and Engineering, Menai, NSW, 2234, Australia

Received 8 March 2001 and Received in final form 18 June 2001

Abstract. The magnetic structure of RFe_6Ga_6 intermetallic compounds with R = Y, Ho have been determined by neutron powder diffraction, ^{57}Fe Mössbauer spectroscopy, AC susceptibility, TGA (Thermo-Gravimetric Analysis) and magnetization measurements. Both compounds crystallize in the tetragonal $ThMn_{12}$ structure (space group I4/mmm) with the magnetic structure of YFe_6Ga_6 consisting of a simple ferromagnetic alignment of Fe moments in the basal plane with a Curie temperature of 475(5) K. Gallium atoms are found to fully occupy the 8i site, with Fe and Ga atoms equally distributed over the 8j site, whilst Fe atoms fully occupy the 8f site. The average Fe moments are 1.68(10) μ_B and 1.46(10) μ_B at 15 and 293 K, respectively. The average room temperature Fe magnetic moments determined by neutron diffraction are in overall agreement with the average Fe moment deduced from Mössbauer spectroscopy and bulk magnetization measurements on this compound. The magnetic anisotropy of the compound $HoFe_6Ga_6$ is also planar in the temperature range 6–290 K, with Ho magnetic moments of 9.28(20) μ_B and 2.50(20) μ_B at 6 K and 290 K, respectively, coupled anti-ferromagnetically to the Fe sublattice and a Curie temperature of 460(10) K. The magneto-crystalline anisotropies of both compounds are comparable at low temperatures.

PACS. 75.50.Gg Ferrimagnets – 75.30.Gw Magnetic anisotropy – 75.25.+z Spin arrangements in magnetically ordered materials (including neutron and spin-polarized electron studies, synchrotron-source X-ray scattering, etc.)

1 Introduction

Many ternary Rare-Earth (R) transition metal (T) intermetallic compounds which crystallize in the tetragonal $ThMn_{12}$ structure (Space Group I4/mmm, $Z = 2$ [1]) have potential for applications as high-performance permanent magnet materials [2]. The most intensively investigated compounds of this type are of the Fe and Co rich compositions $RFe_{12-x}M_x$ and $RCo_{12-x}M_x$ (M = Ti, V, Cr, Al, Si, Mo, W). The stability range of the structure is typically $1 < x < 2$, whilst compounds with M = V are known to stabilize up to $x = 4$ [3,4]. The site occupancy of the stabilizing element M has been determined by neutron diffraction for most of the series [5–8]. In general, the stabilizing element preferentially occupies the 8i site. The homogeneity range for compounds with M = Al, Ga occurs at much higher x. For example, $GdFe_{12-x}Al_x$ compounds stabilize in the $ThMn_{12}$ structure for $6 < x < 8$ [9], whilst compounds with Ga, an element in the same periodic group as Al, were shown to be stable for the compositions $8 < x < 6$ [10,11]. For these compounds, Al atoms are also found to occupy the 8i site [12]. This is in variance with claims that stable ternary $RFe_{12-x}Ga_x$ compounds exist for much lower values of x [13,14]. X-ray diffraction and Mössbauer spectroscopy investigations have conclusively demonstrated that for $1 < x < 2$, $RFe_{12-x}Ga_x$ compounds crystallize either in the hexagonal Th_2Ni_{17} or rhombohedral $Th_{12}Zn_{17}$ structures [15]. The Curie temperature, saturation magnetization and magnetic-energy product variation for the entire series of $RFe_{12-x}Ga_x$ compounds ($x < 6$), which stabilize either in the tetragonal $ThMn_{12}$ or orthorhombic $ScFe_6Ga_6$ (Space group Immm [10]) structures, have been reported by Weitzer *et al.* [16]. The Curie temperatures for both series lie at around 500 K, and the highest saturation magnetization (at 5 K) is reported for tetragonal $NdFe_{5.9}Ga_{6.1}$, at 10.8 μ_B/formula unit, with a corresponding Curie point of 480 K. The behaviour of the Fe sublattice is typified by the magnetization data for tetragonal YFe_6Ga_6, with $T_C = 500$ K and a saturation magnetization at 5 K of 8.6 μ_B/formula unit. The Er- and Fe-sublattice moments at 2 and 290 K as well as the Ga-site distribution, obtained from neutron diffraction data, have been recently reported for $ErFe_6Ga_6$ [17]. The relatively low values of the saturation magnetization are strongly indicative of a correspondingly low magnetic moment of Fe in this series.

In order to investigate in microscopic detail the site dependence of Fe moments in the tetragonal variant of

[a] e-mail: moze.oscar@unimo.it

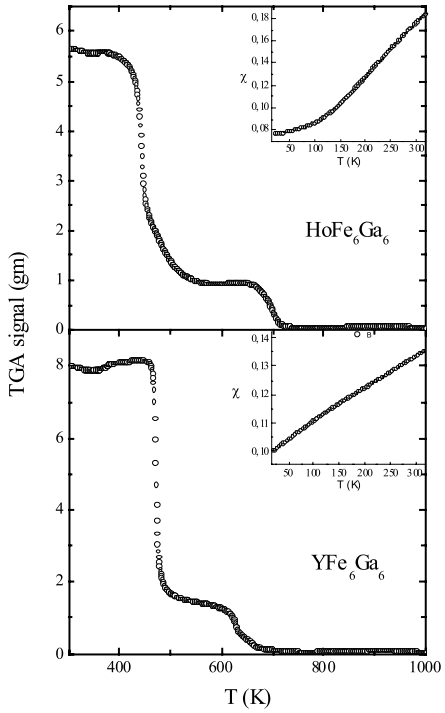

Fig. 1. Thermo Gravimetric Analysis data for YFe_6Ga_6 and $HoFe_6Ga_6$. The temperature dependence of the AC susceptibility for YFe_6Ga_6 and $HoFe_6Ga_6$ is displayed in the inserts.

YFe_6Ga_6, a neutron diffraction investigation of stoichiometric YFe_6Ga_6 has been performed at 15 and 293 K. The distribution of Ga atoms on the 8i, 8j and 8f sites, the Fe moments at these sites as well as the easy magnetization direction have been determined. The present results are in excellent agreement with the neutron diffraction investigation concerning the distribution of Fe and Ga atoms over the available three transition metal sites reported for $ErFe_6Ga_6$. The neutron diffraction data are accompanied by Mössbauer spectroscopy data on YFe_6Ga_6 and TGA (Thermo Gravimetric Analysis) measurements on both compounds. Alternating susceptibility measurements have also been performed on $HoFe_6Ga_6$ and YFe_6Ga_6 in the temperature range 15–320 K, accompanied by high field magnetization measurements, up to 5 T, on both compounds at 5 and 300 K. The temperature dependence of the Ho and Fe sublattice moments, obtained from neutron diffraction data, are also reported for the compound $HoFe_6Ga_6$ in the range 6–290 K.

2 Experimental results and analysis

Stoichiometric 10-gram samples of YFe_6Ga_6 and $HoFe_6Ga_6$ were prepared by arc melting starting materials with at least 3N purity. The resulting ingots were then wrapped in Ta foil and vacuum sealed in quartz tubes and annealed for 3 weeks at 900 °C, followed by a rapid quench in water. X-ray diffraction measurements indicated approximately single-phase materials, isomorphous with the $ThMn_{12}$ structure. Extra diffraction

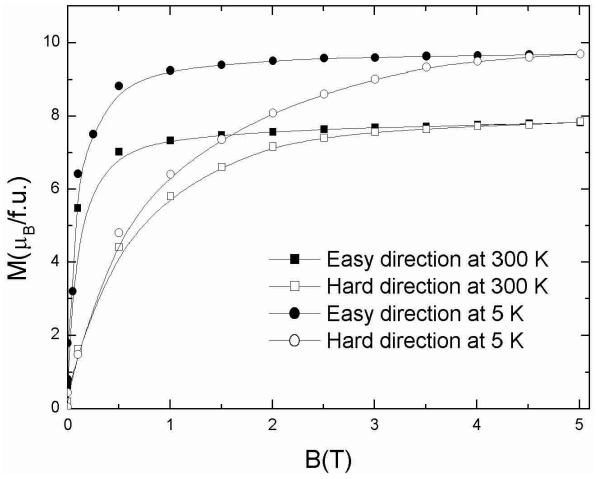

Fig. 2. Field dependence of the magnetization of YFe_6Ga_6 at 5 and 300 K. Lines are guides through the points.

lines indicated the presence of a few percent of an impurity phase, α-FeGa. Neutron powder diffraction measurements were performed on the multi-detector diffractometer MRPD (Medium Resolution Powder Diffractometer), located at the High Flux Australian (HIFAR) Reactor, Lucas Heights, Sydney, Australia. An incident neutron wavelength of 1.6676 Å was used and the data were collected at 15 and 293 K for YFe_6Ga_6 and at 6, 25, 50, 75, 100, 125, 150, 175, 200, 225, 250 and 290 K for $HoFe_6Ga_6$. ^{57}Fe Mössbauer spectroscopy was carried out on a conventional spectrometer in transmission mode, using a ^{57}CoRh source. The spectrometer velocity scale was calibrated with an α-Fe foil. The Curie temperatures, as determined from the TGA measurements performed on a Perkin-Elmer TGA-7, were 475(5) K and 460 (5) K for YFe_6Ga_6 and $HoFe_6Ga_6$ respectively. Both TGA traces show the presence of an impurity phase with an ordering temperature of approximately 700 K. As discussed in detail below, this phase was identified as an α-FeGa alloy, with an approximate composition of 25–30 at.% Ga. AC susceptibility measurements,using a LakeShore Model 7130 closed-cycle AC susceptometer in an applied AC magnetic field of 100 A/m at a frequency of 137 Hz in the temperature range 15–320 K, are displayed in Figure 1, together with the TGA measurements, for both compounds. As can be seen from this figure, there are clearly no spin-reorientation transitions in this range of temperatures. The field dependence of the magnetization along the easy and hard directions for magnetically aligned powders of YFe_6Ga_6 and $HoFe_6Ga_6$, measured at 5 and 300 K, are displayed in Figures 2 and 3 respectively.

Powders sieved in a 20-micron sieve were used for the magnetization measurements. Alignment was performed by rotating the sample around an axis perpendicular to a 1 T alignment field. The grains were then fixed by epoxy resin. Samples prepared in this manner were used for hard direction magnetization measurements. Easy magnetization measurements were performed on free powders. The temperature dependence of the magnetization was also measured on a free powder of $HoFe_6Ga_6$, in an applied

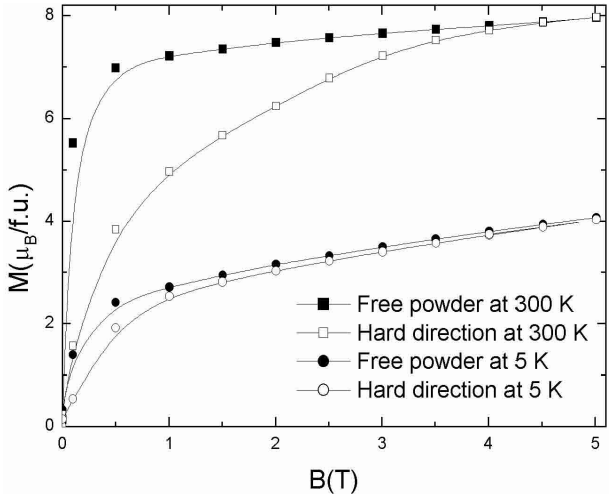

Fig. 3. Field dependence of the magnetization of $HoFe_6Ga_6$ at 5 and 300 K. Lines are guides through the points.

field of 0.5 T, from 5 up to 350 K using a quantum design SQUID magnetometer.

Inspection of the neutron diffraction profiles revealed the presence of a cubic impurity phase (already revealed by X-ray diffraction), in addition to reflections characteristic of the $ThMn_{12}$ structure (lines with Miller indices $h+k+l=2n$). The neutron data reported here were analyzed by the Rietveld technique [18], using the FULLPROF [19] and PRODD [20] suite of programs developed for analysis of neutron and X-ray powder diffraction data. The following neutron scattering lengths were used in the refinement: $b_Y = 0.775 \times 10^{-12}$ cm, $b_{Ho} = 0.801 \times 10^{-12}$ cm, $b_{Fe} = 0.954 \times 10^{-12}$ cm and $b_{Ga} = 0.72888 \times 10^{-12}$ cm, with dipolar approximations for the magnetic form factor for metallic Fe and Ho used in the refinements [21].

The structural model used in the refinements was that of $ThMn_{12}$, *i.e.* R atoms at 2a sites, (0,0,0) and Fe and Ga atoms initially placed in equal proportions at 8i ($x \sim 0.34$, 0, 0), 8j ($x \sim 0.28$, 1/2, 0) and 8f (1/4, 1/4, 1/4) sites. This is the structural model obtained from refinement of the compound $ErFe_6Ga_6$ in the paramagnetic phase [17]. A cubic phase of Fe was used as the impurity phase. Values for the Fe magnetic moments on each sublattice were initially fixed at 1.5 μ_B per Fe atom with the easy magnetization direction along the *c*-axis. After refinement of an overall scale factor, lattice, positional and an overall isotropic temperature factor, the Ga occupancy on each sublattice was varied. The refined Fe and Ga site occupancies were absolutely identical to those obtained for the compound $ErFe_6Ga_6$, which show that Fe and Ga atoms are equally distributed on the 8j sites, Fe fully occupies the 8f site and Ga fully occupies the 8i site. The Fe magnetic moment magnitudes and orientations were refined as a last step. A best agreement was obtained with Fe moments aligned in the basal plane at both temperatures. The calculated average Fe moment of $1.68(24)\mu_B$ for YFe_6Ga_6 at 15 K, obtained from the refined planar Fe moments at 8j and 8f sites at 15 K, $1.96(36)\mu_B$ and $1.55(16)\mu_B$ respectively, is in excellent agreement with a value of $1.6\mu_B$/Fe obtained from macroscopic magnetization data [16,17]. A similarly good agreement is observed for the room temperature magnetic moment values, with an average of 1.38(24) μ_B/Fe calculated from the neutron data *versus* 1.33 μ_B/Fe obtained from magnetization data. Refinements of the data with Fe moments oriented along the *c*-axis gave unreasonably low values of the Fe moments at 8f and 8i sites in addition to a higher *R* factor. The phase fractions of RFe_6Ga_6 and α-Fe were also obtained with a two-phase refinement of the neutron diffraction data for both compounds. The refined phase fractions of the impurity were 6 and 9 wt.% for YFe_6Ga_6 and $HoFe_6Ga_6$, respectively. Best agreement with the observed data was obtained with Fe moments oriented perpendicular to the *c*-axis for YFe_6Ga_6. Overall refinements at 15 and 293 K are tabulated in Table 1, whilst observed, calculated and difference profiles are displayed in Figure 4.

Table 1. Results of Rietveld profile refinements of neutron diffraction data for YFe_6Ga_6 at 15 and 293 K. B_{ov} are overall individual isotropic temperature factors. Y atoms are located at 2a (0, 0, 0), Fe at 8f (1/4, 1/4, 1/4), Ga at 8i (x_1, 0, 0) with Fe and Ga equally distributed over the 8j (x_2, 1/2, 0) site. Quality of fit values are tabulated at the bottom of the table. Errors refer to Estimated Standard Deviations calculated by the Rietveld refinement procedure.

	15 K	293 K
a (Å)	8.57793(54)	8.61825(33)
c (Å)	5.06544(38)	5.09178(22)
x_1 (8i)	0.3365(6)	0.3402(3)
x_2 (8j)	0.2853(5)	0.2802(3)
B_{ov}, (Å^2)	0.10(4)	0.43(4)
μ_{Fe} 8j (μ_B)	1.96(36)	1.48(24)
μ_{Fe} 8f (μ_B)	1.55(16)	1.34(11)
$\mu_{average}$ (μ_B)	1.68(22)	1.54(15)
R_{wp} (%)	10.46	5.40
R_{exp} (%)	7.83	4.28
χ^2	1.78	1.59

Displayed in Figure 5 is the fitted Mössbauer spectrum measured for YFe_6Ga_6 at 295 K. There are three sites available to the Fe in the $ThMn_{12}$ structure but the spectrum is complicated by the fact that the magnetic order is in the basal plane, which will split crystallographically equivalent sites, due to the effect of dipole fields. A further complication arises from the presence of Ga which leads to a distribution of nearest-neighbour environments at the Fe sites. For these reasons, the spectrum was fitted with the minimum number of magnetically-split sextets required to obtain a good fit and hence concentration was focussed on only the average ^{57}Fe hyperfine field which can be determined quite accurately despite the aforementioned effects.

To fit the spectrum, three sextets for the YFe_6Ga_6 phase and an additional broadened sextet for the α-FeGa impurity phase were used. The average ^{57}Fe isomer shift

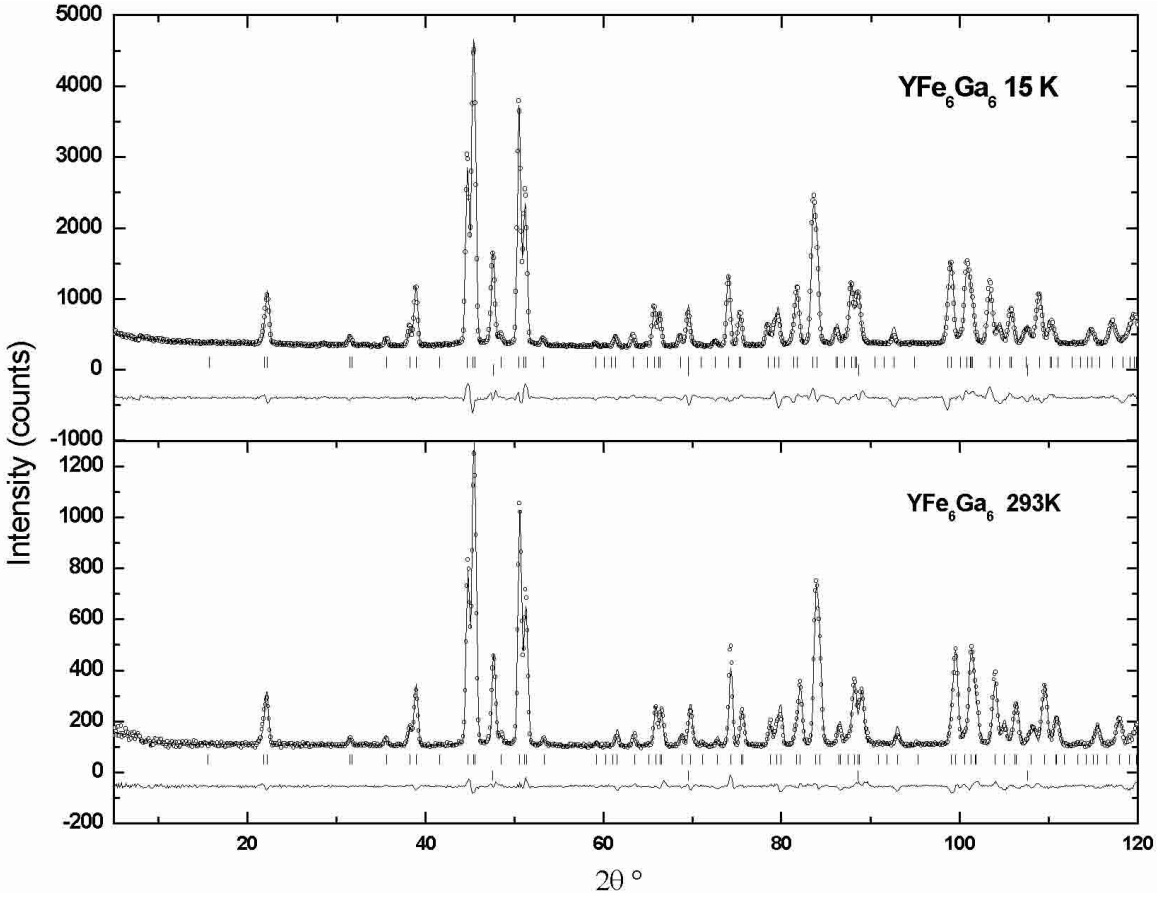

Fig. 4. Observed, calculated and difference neutron powder diffraction patterns of YFe_6Ga_6 at 15 K and 293 K. Tickmarks indicate calculated peak positions for the main phase (top) and those for the Fe-Ga impurity phase (bottom).

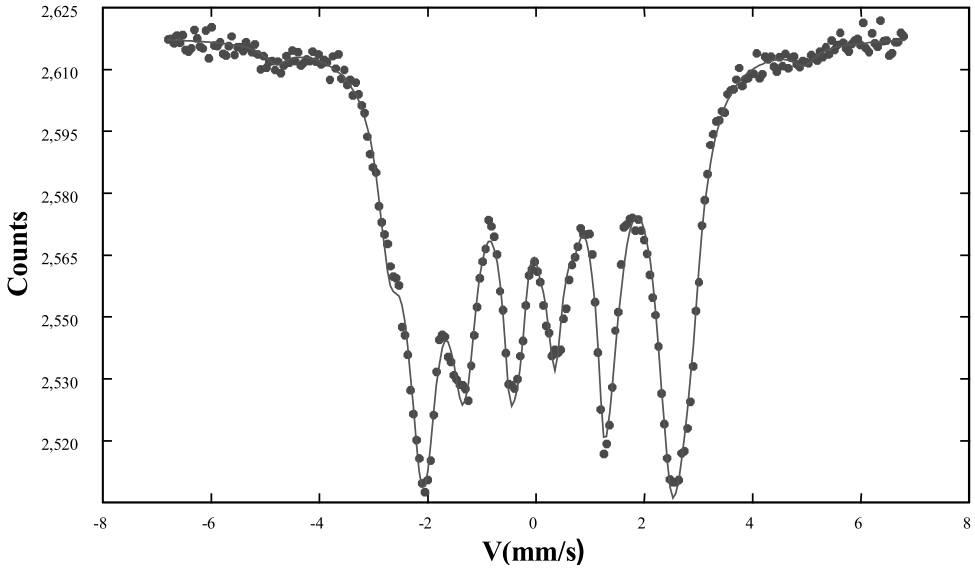

Fig. 5. Fitted Mössbauer spectrum for YFe_6Ga_6 at 293 K.

at 295 K in YFe_6Ga_6 is 0.20(1) mm/s, relative to α-Fe. The average hyperfine field at 295 K is 14.4(3) T, which would correspond to an average Fe magnetic moment of 1.0 μ_B, using the standard conversion factor of 14.7 T/μ_B deduced from α-Fe. However, it is well known that the conversion factor can vary within the range 11–17 T/μ_B in rare-earth intermetallic compounds and can also vary from site to site within a given compound. Thus, the measured hyperfine field gives an average Fe moment of 1.0(3) μ_B.

The Mössbauer spectrum contains a broadened magnetic sextet with a hyperfine field of 30.2 T and a subspectral area of 2.5%. This corresponds to the impurity phase α-FeGa. The reduction in field from the standard value of 33.0 T for α-Fe allows an estimate to be made of the Ga content in the impurity. The Fe-Ga alloy system has been studied by Aldred [22] and Kostetskii and L'vov [24] who showed that the introduction of Ga into α-Fe leads to an increase in Fe moment for Ga concentrations up to about 16 at.%, above which the Fe moment decreases. The measured ^{57}Fe hyperfine field for α-FeGa (30.2 T) corresponds to a Ga content in α-FeGa of approximately 25 at.%. The compound Fe_3Ga has a hyperfine field at 295 K of 31.8 T [24] but the presence of a crystalline Fe_3Ga impurity phase can be clearly ruled out from the neutron diffraction data. The refined cubic lattice parameter of the impurity α-FeGa. phase is 2.921 Å. Using the known variation of the lattice parameter with Ga composition for cubic FeGa alloys [25], this corresponds to an alloy with an approximate composition of $Fe_{70}Ga_{30}$.

The neutron diffraction data at 5 K for $HoFe_6Ga_6$ show a large enhancement of the (110) ($2\theta \sim 16°$), overlapping (101)+(200) ($2\theta \sim 22°$), overlapping (220)+(211) ($2\theta \sim 32°$) and (310) ($2\theta \sim 36°$) reflections, in comparison with the low temperature data for YFe_6Ga_6. In particular, the nuclear and magnetic contributions of the Fe sublattice to the (110) reflection is negligible, and the enhancement of these sets of reflections can clearly be attributed to the ordering of the Ho sublattice. By way of example, the temperature dependence of the integrated intensity for the (110) reflection for $HoFe_6Ga_6$ is displayed in Figure 6.

Rietveld profile refinement of the data for the Ho compound clearly indicate that the anisotropy for this compound is also planar in the temperature range 6–290 K with consistently superior fits obtained with moments oriented in the basal plane rather than along the c-axis. For the data at 6 K, refinements were also performed by fixing the Ho and Fe moments at angles of 25, 50, 60 and 75 degrees to the c-axis. These refinements confirmed that the moments at this temperature (and subsequently at all other measured temperatures) are confined in the plane. Profile refinement factors where similar to those obtained for refinement of the YFe_6Ga_6 data. Observed, calculated and difference profiles at 6 and 250 K for a planar configuration are displayed in Figure 7. (Observed and calculated neutron intensities and structure factors for both compounds are available on request from the authors.) The temperature dependence of the refined Ho and Fe sub-lattice magnetic moments and lattice parameters for $HoFe_6Ga_6$ are displayed in Figures 8, 9 and 10 respectively. Displayed also in Figure 9 is the average Fe sublattice moment deduced from the two individual Fe site moments. The lattice parameters display a simple monotonic increase with temperature.

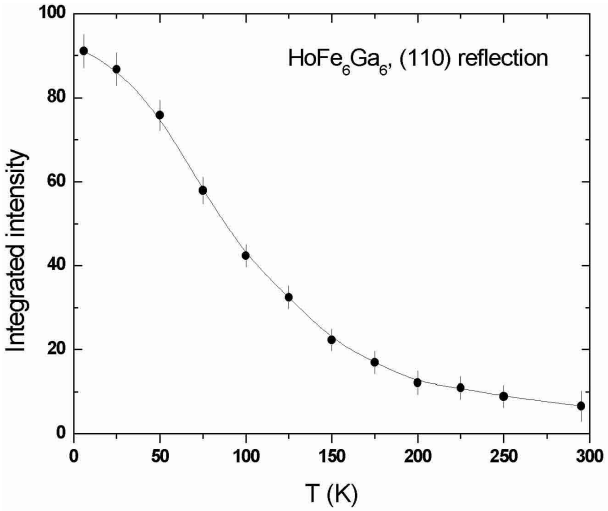

Fig. 6. Temperature dependence of the integrated intensity of the (110) reflection for $HoFe_6Ga_6$. The solid line is only a guide to the eye.

A value of the average molecular field experienced by the Ho moments of 36 T was deduced by fitting the temperature dependence of the Ho moment using a Brillouin function. A constant molecular field value (obtained from a scaling of the temperature dependence of the average Fe moment) was used in the Brillouin function. The assumption of a constant molecular field value is reasonable because the temperature dependence of the Fe moments is fairly constant over the measured range of temperatures. In this fitting procedure, the fitted temperature dependence of the Ho moment is shown as the line through the data points displayed in Figure 8. This value is in excellent agreement with a value of 38 T, deduced from high field magnetization data reported recently for this compound [29].

Displayed in Figure 11 is the temperature dependence of the magnetization for $HoFe_6Ga_6$, measured in an applied magnetic field of 0.5 T, together with the temperature dependence calculated from the neutron diffraction data. Both curves clearly show the classical behaviour expected for a ferri-magnet, but the bulk magnetization data are corrupted by the presence of the Fe-Ga impurity, which adds to the magnetization of the ferrimagnetic $HoFe_6Ga_6$ phase, over the temperature range 5 to 300 K, an almost constant value of approximately 2.5 μ_B/formula unit. A similar behaviour is observed in the magnetization curves of Figures 2 and 3. Taking the presence of this impurity into account and considering the quoted uncertainties in the Ho and Fe magnetic moments as determined by neutron diffraction, the agreement between the bulk and neutron result is satisfying.

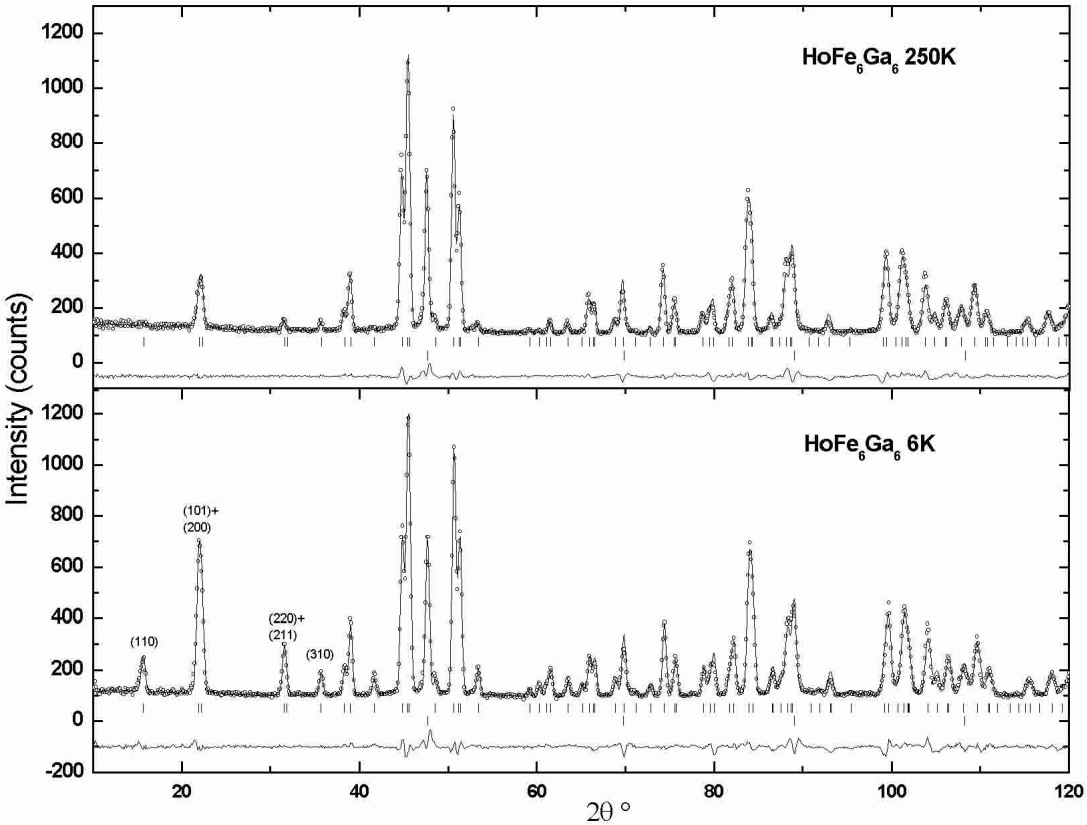

Fig. 7. Observed, calculated and difference neutron powder diffraction patterns of $HoFe_6Ga_6$ at 6 and 250 K. Tickmarks indicate calculated peak positions for the main phase (top) and those for the Fe-Ga impurity phase (bottom).

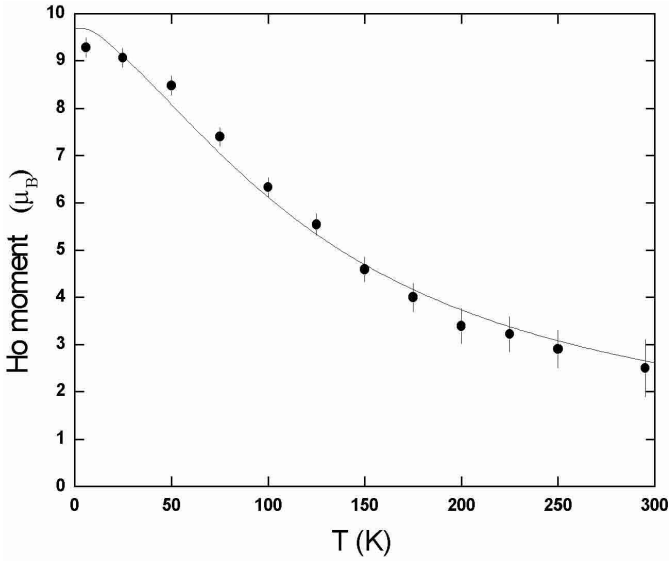

Fig. 8. Temperature dependence of the refined Ho magnetic moment in $HoFe_6Ga_6$ together with the fitted Brillouin function dependence of the Ho moment.

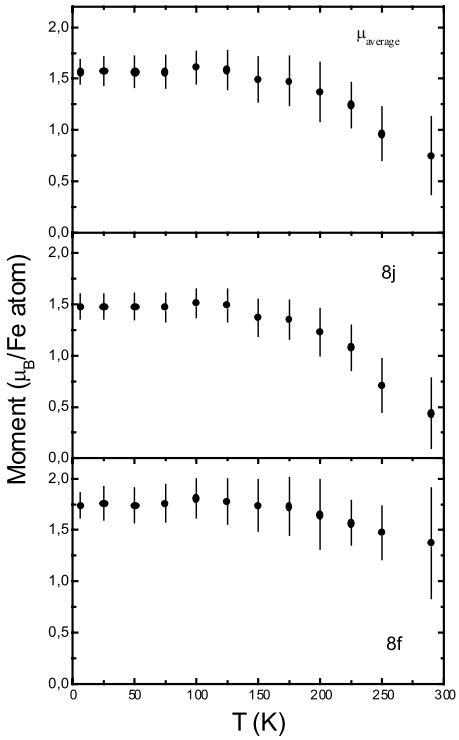

Fig. 9. Temperature dependence of the refined Fe magnetic moments at 8f and 8j sites together with the average Fe moment in $HoFe_6Ga_6$.

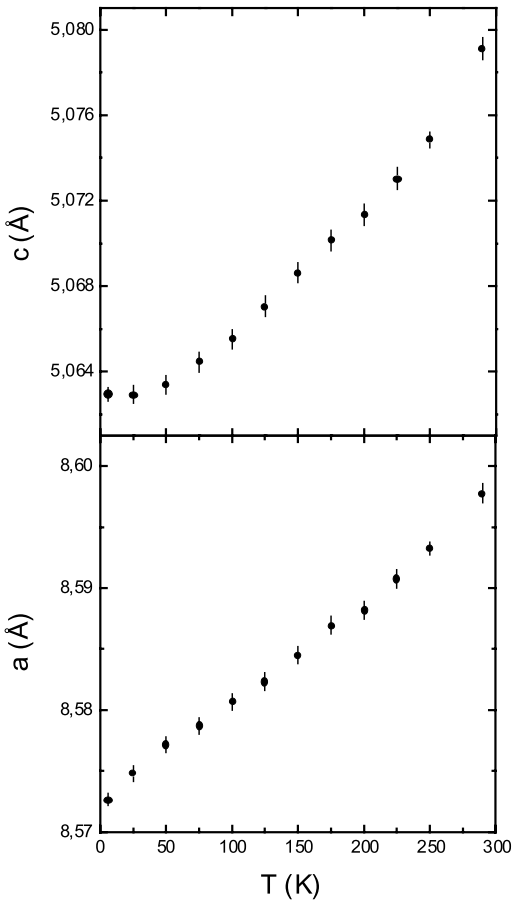

Fig. 10. Temperature dependence of the refined lattice parameters for $HoFe_6Ga_6$.

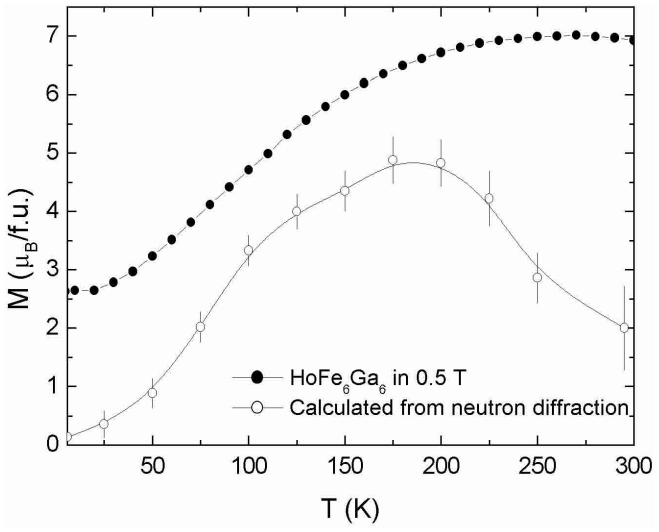

Fig. 11. Temperature dependence of the bulk magnetization measured in a 0.5 T field, together with the bulk magnetization calculated from refinement of neutron diffraction data, for $HoFe_6Ga_6$. The solid lines through the points are guides to the eye.

3 Discussion

Size effects as well as enthalpy considerations both appear to play a role in determining the site preference of M atoms in $RFe_{12-x}M_x$ compounds. This tendency is repeated in RFe_6T_6 compounds with T = Al, Ga where the site occupancy of Al [12] is in good overall agreement with the present reported results, as well as those recently reported for the compound $ErFe_6Ga_6$ [17].

The planar anisotropy of the Fe sublattice is unambiguously confirmed by the present neutron diffraction investigation of the compound YFe_6Ga_6, in agreement with bulk magnetization studies [16] and a neutron diffraction investigation of $ErFe_6Ga_6$ [17]. The largest Fe moment in YFe_6Ga_6 is observed for the 8j site, which is also occupied by Ga, whilst the Fe moment at 8f sites is much lower. The average Fe moment, as deduced from neutron diffraction, is in excellent accord with bulk magnetization measurements. The present neutron diffraction investigation needs to be closely compared with a recent neutron diffraction investigation of $ErFe_5Al_7$, in which a zero Fe magnetic moment is reported for the mixed 8j site, and no long-range magnetic order is displayed [26]. These results indicate a strong dependence of the stability of Fe moments on the local environment around Fe sites. This dependence on local environment appears to be markedly different between compounds with Ga and Al. Magnetization measurements on $TbFe_5Ga_7$ show that this compound orders at about 400 K, which means that the Fe sublattice is ordered magnetically [27].

The Ho moment at low temperatures in $HoFe_6Ga_6$ is reduced by approximately 10% from its free-ion value, a reduction which can be attributed to the crystal field interaction, and the overall easy magnetization direction for this compound is found to be planar for all temperatures up to room temperature. Under the assumption of a rigid coupling between the rare-earth and Fe-sublattice moments and dominant exchange interactions, the relationship between the temperature dependence of the phenomenological anisotropy constants for the rare-earth ion in the free-energy expansion for the magneto-crystalline anisotropy (ignoring two extra terms which describe the anisotropy in the basal plane):

$$E(T) = K_1(T)\sin^2\vartheta + K_2(T)\sin^4\vartheta + K_3(T)\sin^6\vartheta \quad (1)$$

and the thermal averages of the crystal field Stevens operators O_n^m [28]:

$$K_1(T) = -\left[\frac{3}{2}B_2^0\langle O_2^0\rangle + 5B_4^0\langle O_4^0\rangle + \frac{21}{2}B_6^0\langle O_6^0\rangle\right]$$

$$K_2(T) = \frac{7}{8}\left[5B_4^0\langle O_4^0\rangle + 27B_6^0\langle O_6^0\rangle\right]$$

$$K_3(T) = -\frac{231}{16}B_6^0\langle O_6^0\rangle \quad (2)$$

predict that Ho should display an anisotropy different from that observed for Er in RFe_6Ga_6 compounds. The 2nd, 4th and 6th-order Stevens coefficients α_J, β_J and γ_J

for Ho are almost equal in magnitude but opposite in sign to those of Er, which clearly means that the anisotropy of the Ho sub-lattice should be non-planar at low temperatures. In light of the fact that the $ErFe_6Ga_6$ compound is planar at low temperatures, the present neutron results imply a very weak anisotropy of the R sublattice at low temperatures in this particular series of rare-earth intermetallic compounds, with the planar anisotropy of the Fe sublattice dominating the overall anisotropy in both compounds. On the other hand, magnetization measurements reported for $TbFe_6Ga_6$ report a large planar anisotropy for this compound at low temperatures [27]. The planar anisotropy reported for YFe_6Ga_6 at 5 K is much lower, at approximately 4 T, as can be seen from Figure 3. The accompanying planar anisotropy of $HoFe_6Ga_6$ is also relatively weak (see Fig. 4) and comparable in magnitude to YFe_6Ga_6. The inter-sublattice coupling constants for RFe_6Ga_6 compounds with R = Gd, Dy, Ho, Er and Tm have been recently investigated [29]. These measurements are consistent with the model proposed in the analysis of the neutron data presented here, *i.e.* a complete antiparallel coupling between Ho and Fe sublattices. The value of the molecular field experienced by the Ho moments, as deduced from the high field magnetization data, 38 T, is in good accord with a value of 36 T obtained from a fit of the temperature dependence of the Ho moment, as reported in this present work.

In conclusion, neutron diffraction measurements on the tetragonal compounds YFe_6Ga_6 and $HoFe_6Ga_6$ have shown that the Fe and Ho anisotropy is planar for both compounds at low temperatures, as well as at room temperature. A ferromagnetic behaviour is observed for YFe_6Ga_6 whilst $HoFe_6Ga_6$ is ferrimagnetic. The temperature dependence of the Fe and Ho sub-lattices have been determined and the molecular field experienced by the Ho moments, as determined from a fit of the temperature dependence of the Ho moment, is in agreement with the molecular field determined from high field magnetization data. Magnetization measurements performed on both compounds clearly show that the planar anisotropy for the Ho sub-lattice is comparable to that of the Fe sublattices.

The authors gratefully acknowledge provision of neutron scattering facilities by ANSTO. Financial support by the Italian MURST National Research Program "Alloys and Intermetallic Compounds: Thermodynamics, Physical Properties, Reactivity" is gratefully acknowledged. This work is part of the research program of the Stichting voor Fundamenteel Onderzoek der Materie (FOM), which is financially supported by the Nederlandse Organisatie voor Wetunschappelik Onderzoek (NWO). R.T. Gramsma is gratefully acknowledged for his assistance in the magnetization measurements.

References

1. J.V. Florio, R.E. Rundle, A.I. Snow, Acta Cryst. **5**, 449 (1952).
2. K.H.J. Buschow, Rept. Progr. Phys. **45**, 1123 (1991); W. Suski, in *Handbook of Magnetic Materials*, edited by K.H.J. Buschow (Elsevier Science, Amsterdam, 1991), Vol. 6, Chap. 1; W. Suski, in *Handbook on the Physics and Chemistry of Rare Earths*, edited by K.A. Gschneidner Jr, L. Eyring (Elsevier Science, Amsterdam, 1996), Vol. 22, Chaps. 149, 143.
3. D.B. de Mooij, K.H.J. Buschow, J. Less Common Metals **135**, 205 (1988).
4. D.C. Zeng, N. Tang, T. Zhao, Z.G. Zhao, K.H.J. Buschow, F.R. de Boer, J. Appl. Phys. **76**, 6837 (1994).
5. O. Moze, L. Pareti, M. Solzi, W.I.F. David, Solid State Comm. **65**, 465 (1988).
6. M. Solzi, L. Pareti, O. Moze, W.I.F. David, J. Appl. Phys. **64**, 5084 (1988).
7. O. Moze, K.H.J. Buschow, Z. Phys. B **101**, 521 (1996).
8. O. Moze, K.H.J. Buschow, J. Alloys Compounds **233**, 165 (1996).
9. X.-Z. Wang, B. Chevalier, T. Berlureau, J. Etourneau, J.M.D. Coey, J.M. Cadogan, J. Less Common Metals **138**, 235 (1988).
10. N.M. Belyavina, V.Ya. Markiv, Dopov. Akad. Nauk. Ukr. RSR B **12**, 30 (1982).
11. I.A. Grini, O.I. Golovanets, R.V. Labunova, Yu.N. Grin, Ya.P. Yarmolyuk, Dopov. Akad. Nauk. Ukr. RSR A **1**, 74 (1983).
12. O. Moze, R.M. Ibberson, K.H.J. Buschow, J. Phys. Cond. Matt. **2**, 1677 (1990).
13. E. Burzo, M. Valeanu, N. Plugaru, Solid State Commun. **83**, 159 (1992).
14. M. Morariu, M.S. Rogalski, M. Valeanu, N. Plugaru, Mater. Lett. **15**, 383 (1993).
15. J.M. Cadogan, H.S. Li, A. Margarian, J.B. Dunlop, Mater. Lett. **18**, 39 (1993).
16. F. Weitzer, H. Hiebl, P. Rogl, Yu. N. Grin, J. Appl. Phys. **68**, 3512 (1990).
17. K. Prokes, R.T. Gramsma, Y. Janssen, E. Brück, K.H.J. Buschow, F.R. de Boer, Eur. Phys. J. B **16**, 429 (2000).
18. H.M. Rietveld, J. Appl. Cryst **2**, 65 (1969).
19. J. Rodriguez-Carvajal, Physica B **192**, 55 (1993).
20. J.P. Wright, J.B. Forsyth, Rutherford Appleton Laboratory Report RAL-TR-2000-12.
21. E.J. Lisher, J.B. Forsyth, Acta Cryst. A **27**, 545 (1971).
22. A.T. Aldred, J. Appl. Phys. **37**, 1344 (1966).
23. I.I. Kostetskii, S.N. L'vov, Phys. Met. Metallogr. **33**, 95 (1972).
24. N. Kawamija, K. Adachi, Trans. Jpn Inst. Metals **23**, 296 (1982).
25. *Phase Diagrams of Binary Iron Alloys*, edited by H. Okamoto (Materials Information Society, 1993), p. 149.
26. W. Schäfer, B. Barbier, I. Halevy, J. Alloys, Compounds **303-304**, 279 (2000).
27. D.P. Middleton, K.H.J. Buschow, J. Magn. Mag. Mater. **157-158**, 385 (1996).
28. J. Rudowicz, J. Phys. C **20**, 6033 (1987).
29. Y. Janssen, R.T. Gramsma, J.C.P. Klaasse, E. Brück, K.H.J. Buschow, F.R. de Boer, Physica B **294**, 208 (2001).